LASER PHYSICS LETTERS

www.lphys.org

Abstract: The invention of metamaterials prompts reconsideration of a number of fundamental physical phenomena and enables a variety of unique properties and functionalities. These include negative refractive index, magnetism at optical frequencies, sub-wavelength resolution, "backward" phase matching conditions for nonlinear optical processes, and even rendering objects invisible – cloaking. In this brief review, recent progress in basic theory, design, fabrication, characterization, and potential applications of optical metamaterials is discussed.

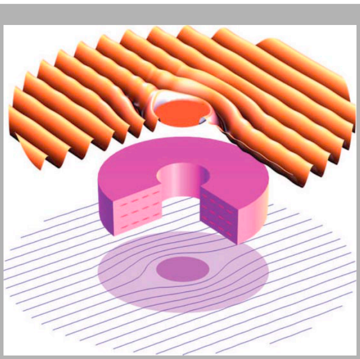

A schematic of two-dimensional non-magnetic cloaking device

Photonic metamaterials

N.M. Litchinitser [1,*] *and V.M. Shalaev* [2]

[1] Department of Electrical Engineering, The State University of New York at Buffalo, Buffalo, New York 14260, USA
[2] School of Electrical and Computer Engineering and Birck Nanotechnology Center, Purdue University, West Lafayette, Indiana 47907, USA

Received: 3 February 2008, Revised: 20 February 2008, Accepted: 23 February 2008
Published online: 3 April 2008

Laser Phys. Lett. **5**, No. 6, 411 – 420 (2008) / **DOI** 10.1002/lapl.200810015

WILEY-VCH

Abstract: The invention of metamaterials prompts reconsideration of a number of fundamental physical phenomena and enables a variety of unique properties and functionalities. These include negative refractive index, magnetism at optical frequencies, sub-wavelength resolution, "backward" phase matching conditions for nonlinear optical processes, and even rendering objects invisible – cloaking. In this brief review, recent progress in basic theory, design, fabrication, characterization, and potential applications of optical metamaterials is discussed.

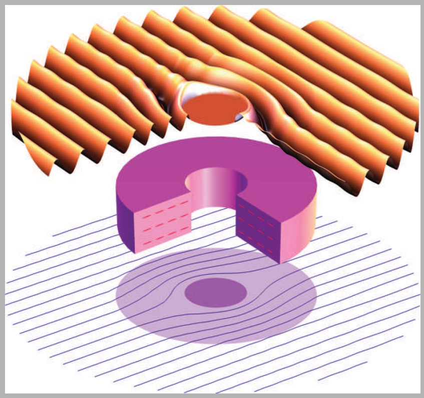

A schematic of two-dimensional non-magnetic cloaking device

Photonic metamaterials

N.M. Litchinitser [1,*] *and V.M. Shalaev* [2]

[1] Department of Electrical Engineering, The State University of New York at Buffalo, Buffalo, New York 14260, USA
[2] School of Electrical and Computer Engineering and Birck Nanotechnology Center, Purdue University, West Lafayette, Indiana 47907, USA

Received: 3 February 2008, Revised: 20 February 2008, Accepted: 23 February 2008
Published online: 3 April 2008

Key words: metamaterials; negative refractive index; superlens; cloaking

PACS: 78.66.Sq, 75.75.+a, 42.65.Wi, 42.79.Bh, 42.79.Gn, 42.65.Ky

1. Introduction: optical metamaterials

Metamaterial technology revolutionized modern optics and photonics by creating nearly unlimited opportunities for engineering material parameters and enabling entirely new linear and nonlinear optical properties and unique functionalities. Originally motivated by "a quest for a superlens" [1], metamaterials gave rise to a plethora of new phenomena and potential applications [2–21], ranging from negative refraction [2–4], total external reflection [5], sub-wavelength waveguides, nanocircuits, antennas, and spectrally selective filters [6–10], to cloaking devices, wave concentrators and rotators [11–17].

Interactions of electromagnetic waves with materials are usually characterized by two parameters – dielectric permittivity $\varepsilon = \varepsilon' + i\varepsilon''$ and magnetic permeability $\mu = \mu' + i\mu''$, where $\varepsilon'(\mu')$ and $\varepsilon''(\mu'')$ are real and imaginary parts of ε and μ, respectively – that explicitly enter Maxwell's equations, or by their product – the index of refraction defined as $n = \pm\sqrt{\varepsilon\mu}$. Surprisingly, despite an evident distinction between various optical materials such as air, water, crystals, semiconductors or metals, their material characteristics occupy a rather limited range of parameters ε and μ. A majority of naturally existing transparent optical materials are characterized by the positive index of refraction, positive dielectric permittivity, and $\mu \approx 1$ implying that the materials are almost nonmagnetic. These restrictions on the range of material parameters in existing materials are mainly imposed by their constituent components – atoms and molecules [22].

Therefore, generalizing the question raised by Victor Veselago about forty years ago [2,23], one could ask: Are there any fundamental physics laws that prohibit other val-

* Corresponding author: e-mail: natasha.litchinitser@gmail.com

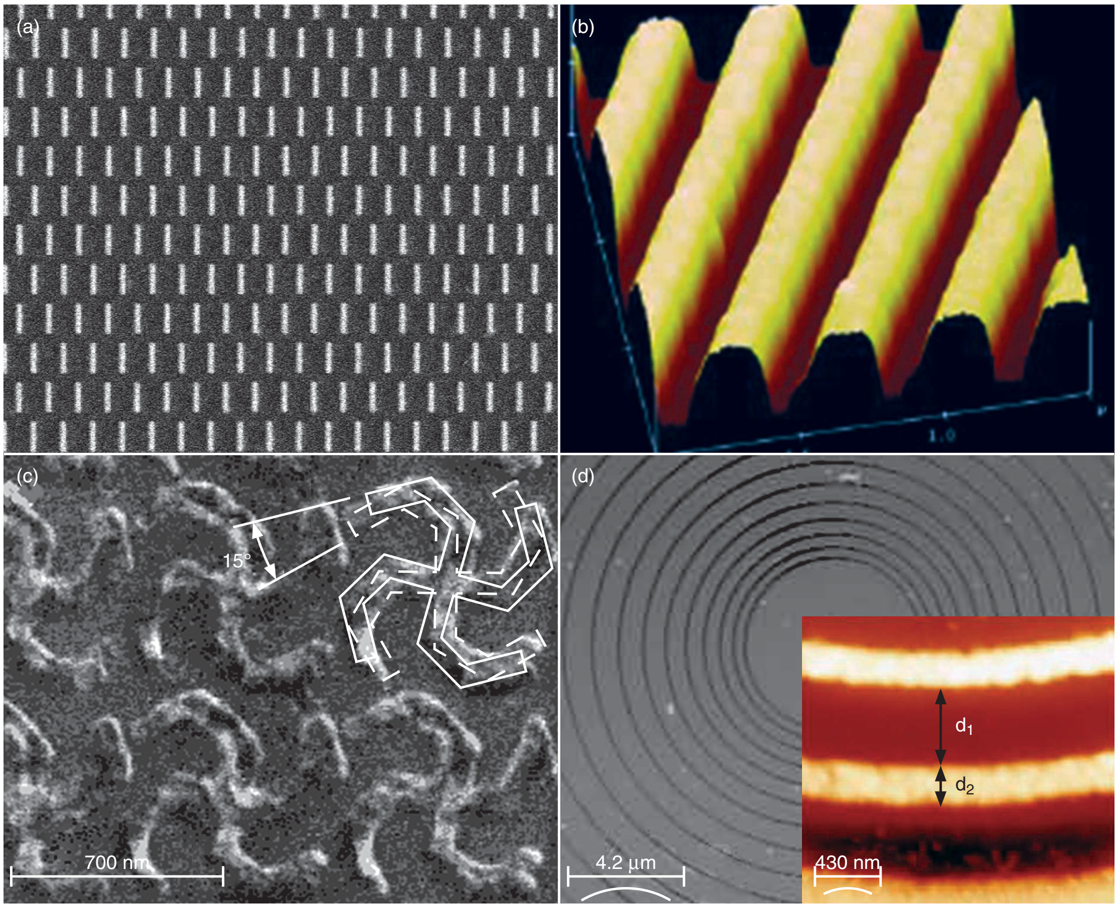

Figure 1 (online color at www.lphys.org) Examples of experimentally demonstrated photonic metamaterials

ues of material parameters or their combinations, in particular, in an optical spectral range?

It turns out that the answer is "no". Theoretical studies combined with the recent progress in nanofabrication proved that in principle any combinations of ε and μ can be realized if the materials are properly engineered. In metamaterials, such engineering is enabled by so-called meta-atoms that substitute natural atoms and molecules. Meta-atoms are engineered structures significantly larger than natural atoms but small compared to the wavelength of incoming radiation. Their electric and magnetic properties can be carefully designed and tuned by changing the geometry, size and other characteristics of meta-atoms [24–26]. Interactions of the electromagnetic waves with meta-atoms may be significantly different compared to that with regular atoms.

Fig. 1 shows several examples of photonic metamaterials. These include (a) one of the first optical metamaterials built of pairs of gold nanorods providing a negative refractive index at 1.5 μm [18], (b) coupled gold nanostrips-based magnetic metamaterial enabling magnetic response across the entire visible range [19], (c) chiral photonic metamaterials [20], and (d) a multilayered structure utilized in the experimental demonstration of the magnifying superlens and a precursor for experimental demonstration of cloaking in the optical range [21].

In this paper, we review recent developments in design, fabrication and applications of magnetic metamaterials opening an opportunity to realization of so-called negative index metamaterials (NIMs) with ε, μ, $n < 0$ and a more general class of engineered homogeneous and inhomogeneous metamaterials.

2. Negative index metamaterials at optical frequencies: design

As discussed in the Introduction, a majority of naturally existing optical materials are non-magnetic. However, it has been recognized for some time that magnetism at optical frequencies may lead to new fundamental physics and novel applications.

One of the most remarkable new classes of materials enabled by bringing magnetism to an optical frequency range is NIMs. In NIMs ε and μ are negative in the same range of frequencies. As a result, the refractive index is also negative. Many of NIMs' unique properties were predicted in the original paper published by Victor Veselago in 1968 [2]. However, the main obstacle to experimental observation of these properties was that NIMs have not been found in nature. It was only more than 30 years after Veselago's original paper that the first experimental demonstrations of NIMs at microwave frequencies were reported [27,28]. In these experiments, following the approach proposed by Pendry et al. [29], NIMs were build of pairs of sub-wavelength concentric SRRs providing negative μ and straight wires responsible for negative ε. This structure can be considered as an *LC*-circuit. The rings form the inductances, while the two slits and the gap between the two rings can be considered as capacitors. The strong magnetic response is achieved by operating in the vicinity of the *LC* resonance of the split ring. A magnetic field, oriented perpendicular to the plane of the rings, induces an opposing magnetic field due to the Lenz's law, which leads to a diamagnetic response resulting in a negative permittivity in a certain range of frequencies. The frequencies of the *LC* resonances in this case are largely determined by the split ring geometry and size rather than by the properties of the metal. At microwave frequencies, metals can be considered as perfect conductors because the skin depth is significantly smaller than the characteristic size of the meta-atom. The same technique of obtaining negative magnetic permeability using SRR has been implemented in the terahertz frequency range by scaling down the dimensions of the split rings [30]. However, adapting this approach to the near-infrared and visible frequencies turned out not to be straightforward for at least two reasons: (i) technical challenges related to the fabrication of resonant structures on the nanoscale, and also (ii) because the resonance frequency saturates as the size of the SRR reduces, and the amplitude of the resonant permeability decreases [31,32].

In the last three years several approaches to the realization of optical NIMs structures have been developed by several groups worldwide [33–42]. One of the first metamaterials with a negative index of refraction at optical frequencies was demonstrated using pairs of metallic nanorods shown in Fig. 1a [18]. The origin of a negative refractive index in a composite material built with such paired nanorods can be understood as follows [43–45]. The electric resonances of individual nanorods originate from the excitation of the surface waves on the metal-air interface. While such surface waves, known as surface plasmon polaritons, cannot be excited with the plane wave in a semi-infinite medium, they are excited in the finite-size nanorods. In a paired nanorod configuration two types of plasmon polariton waves can be supported: symmetric and anti-symmetric. The electric field, oriented parallel to the nanorods, induces parallel currents (symmetric plasmon polariton wave) in both nanorods, leading to the excitation of a dipole moment. The magnetic field, oriented perpendicular to the plane of the nanorods, excites antiparallel currents (anti-symmetric plasmon polariton wave) in the pair of nanorods. Combined with the displacement currents between the nanorods, they induce a resonant magnetic dipole moment. The excited moments are co-directed with the incident field when the wavelength of an incident light is above the resonance, and they are counter-directed to the incident fields at wavelengths below the resonance. The excitation of such plasmon resonances for both the electric and magnetic field components results in the resonant response of the refractive index. In particular, the refractive index can become negative at wavelengths below the resonance. It should be mentioned that simultaneously negative ε and μ is sufficient, but in fact, not a necessary condition for obtaining negative refractive index [46]. Indeed, the following condition $\varepsilon'|\mu| + \mu'|\varepsilon| < 0$ guarantees negative real part of the refractive index. This condition is valid for passive NIMs and indicates that a negative refractive index can be achieved even when $\varepsilon' < 0$ but $\mu' > 0$ provided that $\mu'' \neq 0$, implying that the material is inherently lossy.

The transmission properties of NIMs are often characterized by the figure of merit defined as the ratio of the real and imaginary parts of the refractive index, $F = |n'|/n''$. The larger the FOM, the better the NIMs transmission properties are. Another factor affecting the overall transmission is impedance mismatching. The highest $FOM \approx 3$ for optical NIMs has been demonstrated at $\lambda = 1.4$ μm using the self-supporting fishnet structure consisting of rectangular dielectric voids in parallel metal films [35]. While these proof-of-principle experiments confirmed the possibility of the realization of a negative index of refraction at optical frequencies, the NIMs were significantly lossy, had a very limited bandwidth corresponding to $n < 0$, and were realized only in a form of sub-wavelength films. Therefore, not all potentials of NIMs may be realized in these structures and more advanced designs are still necessary.

3. Novel linear properties and functionalities enabled by NIMs

One of the most fundamental properties of NIMs is antiparallel directions of the phase velocity and the Poynting vector. This property directly follows from Maxwell's equation when both ε and μ are negative. In NIMs, vectors of electric E and magnetic H fields, and a wave vector $\mathbf{k}$ form a left-handed triplet as opposed to a right-handed triplet formed in conventional materials with positive ε and μ. Owing to this distinct feature, NIMs were referred to as left-handed materials by Veselago in his original paper [2].

The second remarkable property of NIMs (that in fact defined their name) is that these materials have a negative index of refraction. As a result, light refracts "negatively" in contrast to conventional, or "positive" refraction [2–4]. It should be stressed that, in general, negative refraction is not equivalent to negative refractive index [47]. Negative refraction associated with NIMs has been demonstrated at microwave frequencies in a metamaterial wedge and in

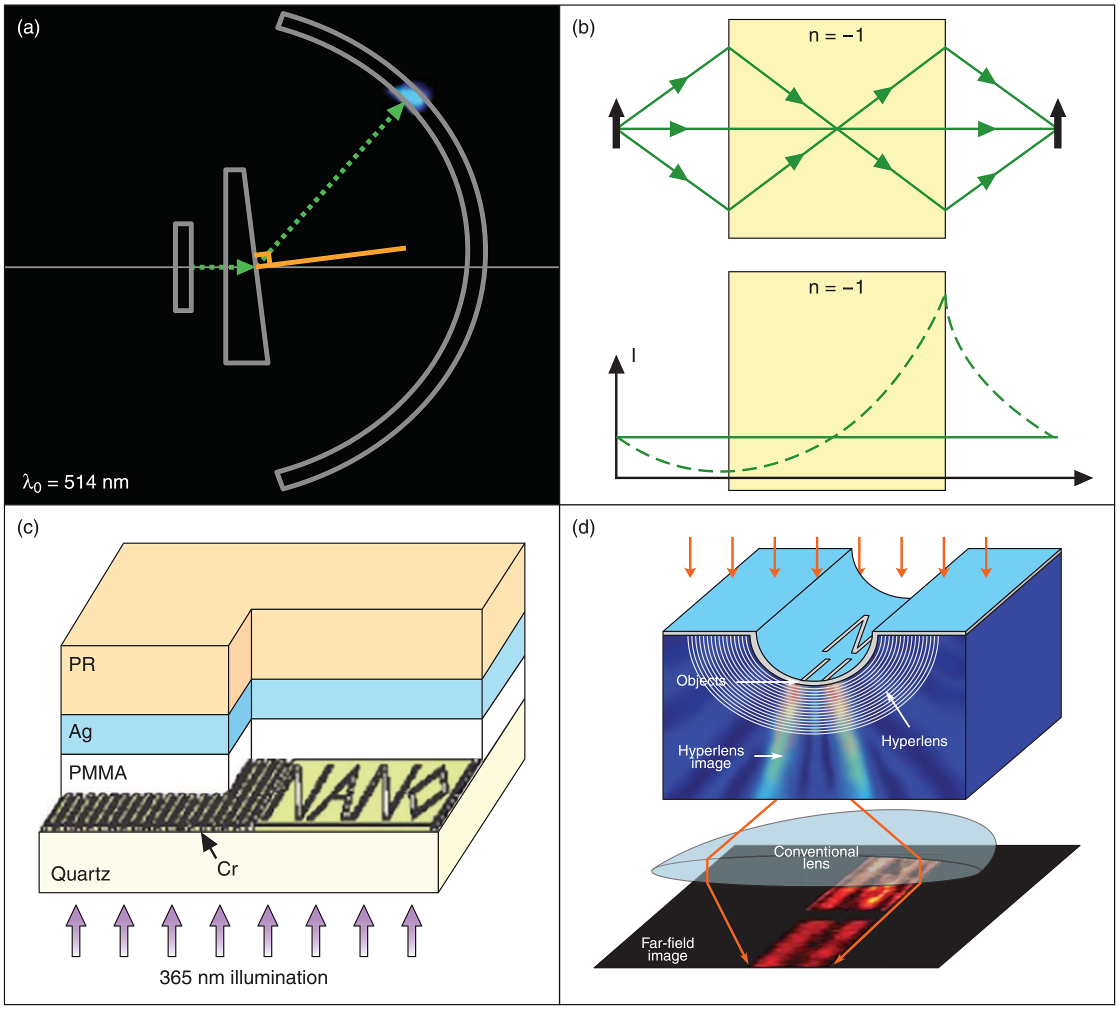

Figure 2 (online color at www.lphys.org) Illustration of unusual optical properties and novel functionalities enabled by NIMs

visible frequency range at the interface between bimetal Au-Si_3N_4-Ag waveguide and a conventional Ag-Si_3N_4-Ag slot waveguide using plasmons as shown in Fig. 2a [4]. Also, negative refraction at optical frequencies was demonstrated in photonic crystals (PC) [48]. However, it should be mentioned that the main limitation of PCs for realization of many unusual phenomena associated with negative index of refraction is that the size of their characteristic features is comparable to the wavelength of light. On the contrary, optical metamaterials with a feature size much smaller than the wavelength of light are predicted to enable many truly remarkable phenomena. However, currently optical metamaterials are only available in the form of subwavelength thin films, thus permitting the measuring of a phase advance but not the negative refraction per se.

The third fundamental characteristic of NIMs is the inherent frequency dependence of both ε and μ. This property originates from the fact that NIMs are resonant structures, i.e. negative ε and μ occur in a close proximity of electric and magnetic resonances. As a result, the refractive index is negative only in a limited range of frequencies. In fact, the same material may act as a NIM in one range of frequencies, and as a conventional positive index material (PIM) at other frequencies.

In addition to extraordinary fundamental physical properties, NIMs give rise to unique functionalities and device applications. A very unusual property of NIMs is the possibility of imaging using a flat slab of NIM with $n = -1$ surrounded by the conventional medium with $n = 1$. Moreover, under the appropriate conditions the NIM slab not only re-focuses the propagating field components, but also re-amplifies the evanescent field components that decay exponentially with distance from source (Fig. 2b) through the excitation of plasmon resonance on the NIM surfaces. These evanescent field components responsible for the imaging of the high frequency and correspondingly small-scale features of the object cannot be restored by conventional lenses, inevitably limiting its resolution. Thus, at least in an ideal (lossless) case, an imaging system based on a NIM slab, named a "superlens" by Pendry [1], has the potential for significantly improved resolution in the image plane. Unfortunately, a superlensing effect is extremely sensitive to losses in the NIM slab.

A somewhat simpler version of the superlens, a so-called "poor man's superlens" shown in Fig. 2c has been proposed for applications that involve distances that are much smaller than a wavelength [49–51]. In this case, a sub-wavelength resolution can be realized using single-negative ($\varepsilon < 0$) materials such as metals at the UV or visible frequencies. In particular, it was proposed to use sub-wavelength sheets of silver to obtain near-field focusing for TM-polarized light. Following this strategy, a sub-wavelength imaging on a scale of a few tens of nanometers has been demonstrated experimentally. Improved ($\lambda/20$) resolution was achieved further when silver was replaced by silicon carbide, which provides a better performance in terms of losses [52]. However, an inherent limitation of this type of lens is its near-field performance.

A promising solution towards far-field imaging was proposed independently by Narimanov and Engheta [53,54]. The basic idea of a so-called hyperlens is shown in Fig. 2d. This device is based on recently proposed strongly anisotropic metamaterials that feature opposite signs of the two permittivity tensor components [55–57]. Such metamaterials have been shown to support propagating waves with very large wave numbers (that would evanescently decay in ordinary dielectrics) [55,58]. Therefore, instead of re-amplifying and re-focusing the evanescent field components as Pendry's superlens does, a hyperlens converts those evanescent waves into propagating waves. Once all the components are propagating waves, they can easily be imaged by a conventional lens (microscope) in the far field. Finally, Zhang's group demonstrated another type of far-field superlens by using surface grating to convert evanescent waves into propagating waves [59].

It is noteworthy that the majority of unique properties of NIMs most efficiently reveal themselves when NIMs are combined with conventional positive index materials. As will be illustrated in the next section, NIMs and PIMs can be combined either spatially or spectrally.

4. Nonlinear optics in NIMs

In addition to unusual linear properties, combinations of PIMs and NIMs fundamentally change nonlinear optical interactions. It has been suggested that nonlinear NIMs can be created by inserting nonlinear elements into the slots of SRR [60]. For example, in microwave range the nonlinear response has been obtained by inserting diodes into the SRR [61].

As mentioned in the introduction, both ε and μ are frequency dependent in NIMs. Therefore, the same material can reveal negative-index properties at one wavelength and positive-index properties at another wavelength, forming a basis for fundamentally new regimes of nonlinear optical interactions.

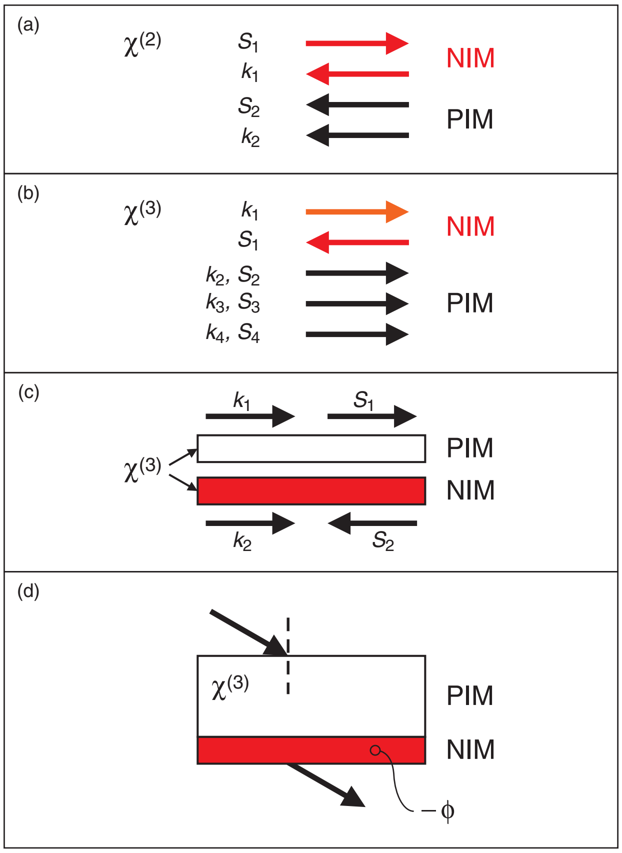

Figure 3 (online color at www.lphys.org) New regimes of nonlinear effects in NIMs with $\chi^{(2)}$ and $\chi^{(3)}$ nonlinearities

In particular, one of the most fundamental properties of NIMs – antiparallel wave and Poynting vectors results in many extraordinary nonlinear optical phenomena, including unusual Manley-Rowe power conservation relations and "backward" phase-matching conditions enabling new regimes of second-harmonic generation (SHG) [62–67] and optical parametric amplification (OPA) [67–71], surface and guided waves regimes unattainable in conventional waveguides [72,73], and new types of temporal and spatial solitons [74–78].

4.1. Second-harmonic generation

The basic idea of backward phase-matching is illustrated in Fig. 3a. It is assumed that the metamaterial is a NIM at the fundamental frequency ω_1 and it is a PIM at the second-harmonic frequency ω_2. If the energy flow of the fundamental frequency travels from left to right, the phase of the wave at the same frequency should move in the opposite direction, that is, from right to left. The phase-matching requirement $k_2 = 2k_1$ can be satisfied if the phase of the second harmonic also travels from right to left. Since the second harmonic propagates in the PIM, its energy flow is co-directed with the phase velocity and, therefore, the energy propagates from right to left as well, as shown in Fig. 3a. On the contrary, in the conventional PIM materials, wave and Poynting vectors propagate in the same direction at both fundamental and second-harmonic frequency and backward phase-matching generally does not occur.

One of the important differences between the SHG in the NIM and PIM cases is reflected in the Manley-Rowe relations given by $|A_1|^2 - |A_2|^2 = C$, where A_1 and A_2 are slowly varying amplitudes of the fundamental and second-harmonic waves, respectively. Therefore, while in the conventional PIM case, the Manley-Rowe relations require that the sum of the squared amplitudes is constant [66,67], in the NIM case their difference is constant. This unusual form of Manley-Rowe relations in NIMs is a direct result of the fact that the Poynting vectors for the fundamental and the second harmonic are antiparallel, while their wavevectors are parallel.

It is noteworthy that the boundary conditions for the fundamental and second-harmonic waves in the NIM case are specified at opposite interfaces of the slab of a finite length L in contrast to the PIM case, where both conditions are specified at the front interface. Owing to such boundary conditions, the conversion at any point within the NIM slab depends on the total thickness of the slab. In the limit of a semi-infinite NIM, both fundamental and second-harmonic waves disappear at infinity and, therefore, a 100% conversion efficiency of the incoming wave at the fundamental frequency to the second harmonic frequency propagating in the opposite direction is expected. As a result, the NIM slab acts as a nonlinear mirror [65,66].

4.2. Optical parametric amplification

An important potential application of backward-phase matching realized in NIMs is the compensation of losses. As discussed above, losses are one of the major obstacles that delay many practical applications of optical NIMs. The basic idea of loss compensation using the OPA is to use the electromagnetic waves with the frequencies outside the negative index frequency range to provide the loss-balancing OPA at frequencies corresponding to a negative index of refraction. Two basic approaches for loss compensation using the OPA have been investigated theoretically. One possibility relies on the $\chi^{(2)}$-nonlinearity of the NIM [68]. In this case, a strong pump field at frequency ω_3 interacts with the signal at frequency ω_1. As a result, the signal is amplified, and a new wave, an idler, at frequency $\omega_2 = \omega_3 - \omega_1$ is generated that contributes back to ω_1.

An alternative approach does not require a strong nonlinear response of the meta-atoms. Instead, it employs embedded four-level centers that can be controlled independently from the NIM parameters, resulting in a possible realization of frequency-tunable transparency windows in NIMs [71]. This technique is based on a four-wave interaction process in a medium with the $\chi^{(3)}$ (cubic)-nonlinearity. In this case, two pump fields at frequencies ω_3 and ω_4 and a signal field at ω_1 combine to generate an idler at $\omega_2 = \omega_3 + \omega_4 - \omega_1$, which is amplified and contributes back to the signal field through the four-wave mixing process, which results in strongly enhanced OPA.

Fig. 3b illustrates the OPA based on $\chi^{(3)}$-nonlinearity. Here, it is assumed that the signal propagates in the NIM, while the pumps and the idler correspond to the PIM frequency range. Generally, both quadratic and cubic parametric amplification processes strongly rely on phase-matching between the interacting waves. As a result of the opposite directionality of the phase and energy velocities, backward phase-matching takes place in both quadratic and cubic nonlinearity cases. The important advantage of the backward OPA in NIMs is effective distributed feedback, which enables oscillations without a cavity. In the NIM case, each spatial point serves as a source for the generated wave in the reflected direction, whereas the phase velocities of all interacting waves are co-directed. This is also true in the SHG case. Recently, parametric amplification has been demonstrated experimentally in negative index nonlinear transmission line media [70].

4.3. Bistability and gap solitons in spatially combined NIM-PIM structures

Backward waves can also facilitate an effective feedback mechanism in wave-guiding structures. This novel mechanism will be exemplified by a nonlinear coupler with one channel filled with NIM. It turns out that introducing a NIM in one of the channels dramatically changes both the linear and nonlinear transmission characteristics of such a coupler [79–81]. In contrast to the previous case of SHG and the OPA, in a PIM-NIM coupler, PIMs and NIMs are combined spatially as shown in Fig. 3c. While nonlinear couplers made of conventional PIM materials have attracted significant attention owing to their strong potential for all-optical processing applications, they typically lack an important functionality – optical bistability if no external feedback mechanism is introduced. In contrast, it was found that the PIM-NIM coupler exhibits bistable transmission and support gap solitons originating from their inherent property – antiparallel phase and energy velocities in NIM channel and parallel phase and energy velocities in the PIM channel, which results in an “effective” feedback mechanism.

Another important manifestation of negative refractive index is a negative phase shift (phase advance) that was measured in thin films of NIMs in the first experiments [18]. Recently several novel device applications that rely on such phase shifts including miniaturized optical waveguides, resonators and laser cavities, phase compensators/conjugators, and nonreciprocal (diode-like) applications have been proposed [82–86].

Novel regimes of optical bistability and potentially useful nonlinear transmission properties of layered structures containing thin films of NIMs have been identified in a layered structure consisting of a slab of nonlinear PIM and a thin film of linear NIM as shown in Fig. 3d [86]. As previously discussed, the state-of-the-art optical NIMs were realized only in the form of sub-wavelength thin films. While no propagation effects or negative refraction, as such, can be observed in these films, the negative index of refraction reveals itself in a phase advancement (negative phase shift), which is in contrast to the phase retardation (positive phase shift) in conventional PIMs.

The simplest way of introducing nonlinearities to existing NIM films is to place an overlay of nonlinear material such as nematic liquid crystals [25,86,87], with very high nonlinear $\chi^{(3)}$coefficients of $\sim 10^{-9}$ m^2/W, on top of the NIM thin film as shown in Fig. 3d. A nonlinear film itself surrounded by a linear dielectric with a high refractive index can be considered as a resonator and is known to exhibit bistability, when illuminated at an angle close to the angle of total internal reflection. As the incident intensity increases, in the case of self-focusing Kerr nonlinearity, the nonlinear refractive index increases, while the transmission coefficient becomes a multi-valued function of the input flux, leading to the formation of a hysteresis loop. A linear NIM thin film placed next to the nonlinear slab acts as a phase element. Although the layer is very thin, the effect of the phase shift introduced by this layer on the nonlinear optical response of the entire structure turns out to be very significant. As discussed above, the effect of the NIM thin film reveals itself in a phase advance or a negative phase shift. As a result, the total resonator length decreases, implying that the intensity-dependent nonlinear index change required for switching the transmission to the high-transmission state should increase, which is in contrast to the case of PIM thin film. The strong sensitivity of the nonlinear response to the NIM's parameters may be particularly useful for the characterization of NIMs. Finally, it has been shown that the same bilayered structure supports a non-reciprocal transmission; that is, nonlinear transmission characteristics are not symmetric with respect to the direction of light propagation. This property may be particularly useful for developing diode-like applications in NIMs.

5. Inhomogeneous metamaterials: cloaking applications

While originally the entire field of metamaterials was stimulated by the development of NIMs, recently yet another exciting branch of modern optics developed – transformation optics. First applied to the development of the optical cloak [11–17], transformation optics is now considered to be a very general and powerful design tool that offers unparalleled opportunities for controlling light propagation through careful refractive index engineering. Recently, various functionalities and novel device applications enabled by this approach have been proposed, including image-processing operations such as translation, rotation, mirroring and inversion, light concentrators [88–90], impedance-matched hyperlens [91], and others.

The general design strategy using the transformation approach includes two main steps. In the first step, a coordinate transformation of the space with desired property is built. In the next step, a set of material properties that would realize this property of the transformed space in the original space using the following equations

$$\varepsilon^{i'j'} = \left|\det(\Lambda_i^{i'})\right|^{-1} \Lambda_i^{i'} \Lambda_j^{j'} \varepsilon \qquad (1)$$

$$\mu^{i'j'} = \left|\det(\Lambda_i^{i'})\right|^{-1} \Lambda_i^{i'} \Lambda_j^{j'} \mu \quad i, j = 1, 2, 3\,,$$

where it was assumed that the original space is isotopic and transformations are time invariant, and $\Lambda_\alpha^{\alpha'} = \partial x^{\alpha'}/\partial x^\alpha$ are the elements of the Jacobian transformation matrix, is calculated.

Recently, the first theoretical designs and experimental demonstrations of cloaking devices at microwave frequencies, shown in Fig. 4a and Fig. 4b, and a theoretical design of an optical cloak, shown in Fig. 4c, based on the transformation optics approach have been reported. Moreover, very recently a first step toward experimental demonstration of cloaking in the visible range was taken by Smolyaninov et al. [21], who demonstrated a cloaking-like behavior for surface plasmon polaritons, shown in Fig. 4d.

As a point of reference, by an "ideal cloak" we understand a device that renders objects invisible and that is object-independent, macroscopic, operates for non-polarized light and in a wide range of frequencies simultaneously, does not reflect, scatter, or absorb any light, introduce any phase shifts, or produce a shadow. While several approaches making objects invisible have been proposed in the literature [92–97], the approach discussed here, often referred to as "re-direction" approach [11–17], appears to be the most general and, therefore, practical one.

In order to redirect waves around the object, either the space around the object should be deformed, assuming that material properties stay the same, or the material properties should be modified around the object. The former approach is referred to as topological interpretation, while the latter is called a material interpretation. Owing to the form invariance of Maxwell's equations, these two interpretations are equivalent. More specifically, under a coordinate transformation, the form of Maxwell equations should remain invariant while new ε and μ would contain the information regarding the coordinate transformation and the original material parameters.

Using this approach, the first working designs of microware and optical cloaks have been proposed theoretically and demonstrated experimentally. The coordinate transformation that compresses the cylindrical region $0 < r < b$ in space into the shell $a < r' < b$ is given by [11]

$$r' = \frac{b-a}{b} r + a\,, \quad \theta' = \theta\,, \quad z' = z\,. \qquad (2)$$

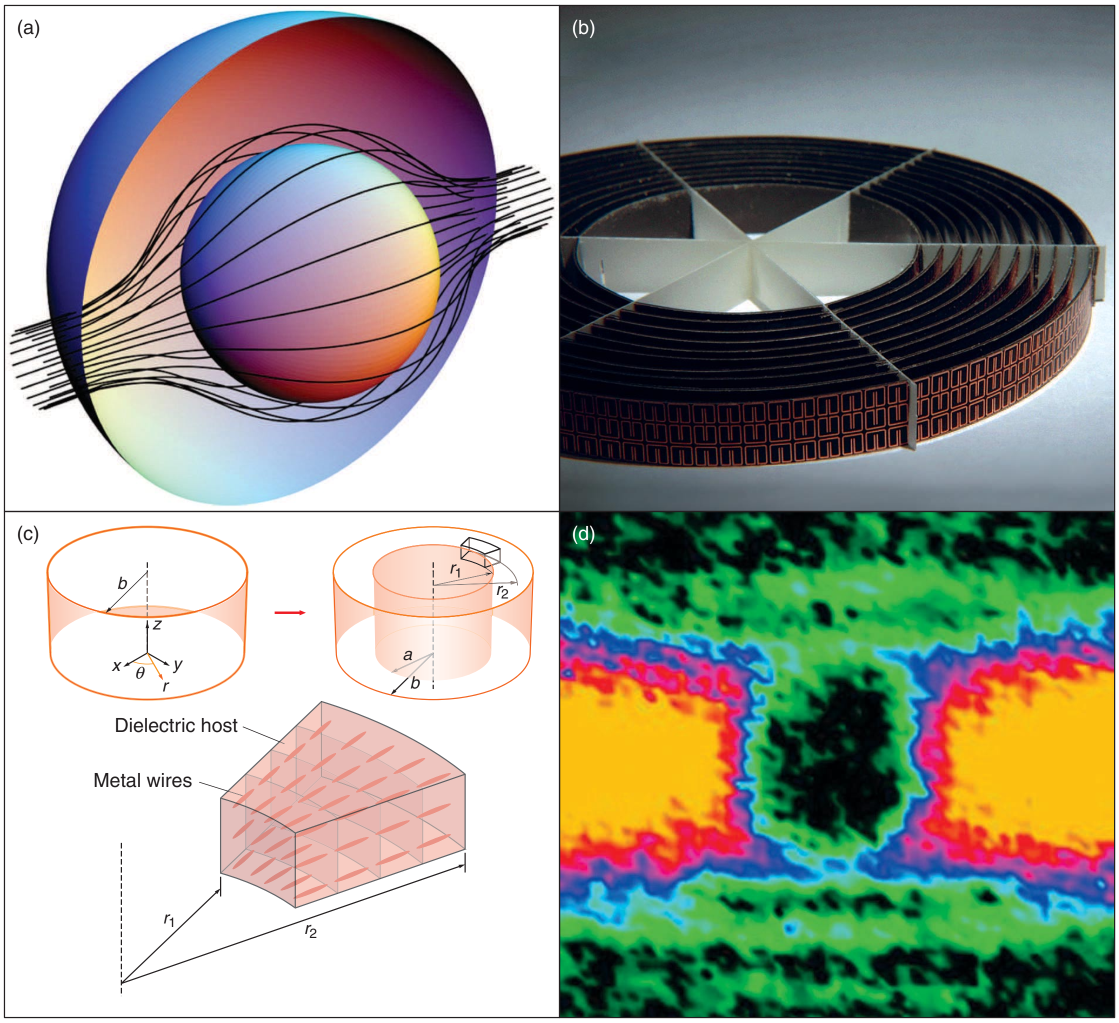

Figure 4 (online color at www.lphys.org) Examples of theoretically proposed and experimentally demonstrated cloaking designs in microwave and visible ranges

The design equations (1) give the following material parameters

$$\varepsilon_r = \mu_r = \frac{r-a}{r}\,, \quad \varepsilon_\theta = \mu_\theta = \frac{r}{r-a}\,, \tag{3}$$

$$\varepsilon_z = \mu_z = \left(\frac{b}{b-a}\right)^2 \frac{r-a}{r}\,.$$

While magnetism at optical frequencies has been demonstrated previously, it is still considered a challenging task that can only be realized in resonant structures with relatively high loss. However, it was realized that an optical cloak for the TM polarization can be built without any magnetism. In this case, Eqs. (3) are replaced with the following set of reduced parameters [16]

$$\mu_z = 1\,, \quad \varepsilon_\theta = \left(\frac{b}{b-a}\right)^2\,, \tag{4}$$

$$\varepsilon_r = \left(\frac{b}{b-a}\right)^2 \left(\frac{r-a}{r}\right)^2\,,$$

A constant, greater than one azimuthal dielectric permittivity component can easily be achieved in conventional dielectrics. A crucial part of the design is the realization of the required radial distribution of dielectric permittivity varying from zero to one. This can be achieved using sub-wavelength metal wires aligned along the radii of the annular cloak shell as shown in Fig. 4c. Other potential implementations of design parameters (4) include chains of metal nanoparticles and thin continuous and semi-continuous strips.

Note that the optical cloak designed using Eqs. (4) is object-independent and does not impose any limitations of the size of the object. However, it is not completely reflection-, scattering-, absorption-, phase shift-, and shadow-free, due to the impedance mismatch related to reduced design parameters (4) and small but non-negligible material absorption. Additionally, it is designed for TM polarization only. Finally, the device is inherently narrowband. Indeed, since the refractive index of the cloaking shell varies from zero to one (as follows from Eq. (4)), a phase velocity of light inside the shell is greater than the velocity of light in a vacuum. While this condition itself does not contradict any law of physics, it implies that the material parameters must be dispersive.

Finally, until recently all cloaking devices designed using the transformation method relied on a linear transformation. Reduced parameters (4) are easier to implement than exact material parameters described by Eqs. (3), but a limitation associated with this set of parameters is that the cloak is not reflectionless. A promising solution to this problem proposed recently [17] is to use a high-order coordinate transformation that eliminates undesired reflections at the outer boundary of the non-magnetic optical cloak.

6. Summary

To summarize, over the last eight years enormous theoretical and experimental progress has been made in the field of metamaterials. Naturally, as in many other areas of science, theoretical research develops faster than its experimental counterpart. To date, many fascinating linear and nonlinear phenomena taking place in metamaterials have been theoretically predicted that still remain to be experimentally demonstrated. Nevertheless, in less than a decade, several phenomena that would undoubtedly have been considered science fiction only a few years ago have been explicitly demonstrated. While further progress in the design and fabrication of metamaterials is required before it becomes a reliable technology, once fully developed, metamaterials technology is likely to revolutionize the imaging, data storage, and telecommunications fields, to name a few.

Acknowledgements The authors acknowledge the support of the Army Research Office through grants W911NF-07-1-0343 and 50342-PH-MUR.

References

[1] J.B. Pendry, Phys. Rev. Lett. **85**, 3966 (2000).
[2] V.G. Veselago, Sov. Phys. Uspekhi **10**, 509 (1968).
[3] A.A. Houck, J.B. Brock, and I.L. Chuang, Phys. Rev. Lett. **90**, 137401 (2003).
[4] H.J. Lezec, J.A. Dionne, and H.A. Atwater, Science **316**, 430 (2007).
[5] B.T. Schwartz and R. Piestun, J. Opt. Soc. Am. B **20**, 2448 (2003).
[6] J. Li and N. Engheta, Phys. Rev. B **74**, 115125 (2006).
[7] N. Engheta, Science **317**, 1698 (2007).
[8] M.G. Silveirinha and N. Engheta, Phys. Rev. B **76**, 245109 (2007).
[9] A. Ourir, A. de Lustrac, and J.-M. Lourtioz, Appl. Phys. Lett. **88**, 084103 (2006).
[10] V.A. Fedotov, P.L. Mladyonov, S.L. Prosvirnin, and N.I. Zheludev, Phys. Rev. E **72**, 056613 (2005).
[11] J.B. Pendry, D. Schurig, and D.R. Smith, Science **312**, 1780 (2006).
[12] U. Leonhardt, Science **312**, 1777 (2006).
[13] U. Leonhardt and T.G. Philbin, New J. Phys. **8**, 247 (2006).
[14] D. Schurig, J.J. Mock, B.J. Justice, S.A. Cummer, J.B. Pendry, A.F. Starr, and D.R. Smith, Science **314**, 977 (2006).
[15] S.A. Cummer and D. Schurig, New J. Phys. **9**, 45 (2007).
[16] W. Cai, U.K. Chettiar, A.V. Kildishev, and V.M. Shalaev, Nature Photonics **1**, 224 (2007).
[17] W. Cai, U.K. Chettiar, A.V. Kildishev, and V.M. Shalaev, Appl. Phys. Lett. **91**, 111105 (2007).
[18] V.M. Shalaev, W. Cai, U.K. Chettiar, H.-K. Yuan, A.K. Sarychev, V.P. Drachev, and A.V. Kildishev, Opt. Lett. **30**, 3356 (2005).
[19] W. Cai, U.K. Chettiar, H.-K. Yuan, V.C. de Silva, A.V. Kildishev, V.P. Drachev, and V.M. Shalaev, Opt. Express **15**, 3333 (2007).
[20] E. Plum, V.A. Fedotov, A.S. Schwanecke, and N.I. Zheludev, Appl. Phys. Lett. **90**, 223113 (2007).
[21] I.I. Smolyaninov, Y.J. Hung, and C.C. Davis, arxiv.org/abs/0709.2862v2.
[22] L.D. Landau, E.M. Lifshitz, and L.P. Pitaevskii, Electrodynamics of Continuous Media (Course of Theoretical Physics, vol. 8), 2nd edition, (Butterworth-Heinemann, Oxford, 1984).
[23] V. Veselago, L. Braginsky, V. Shklover, and Ch. Hafner, J. Comp. Theor. Nanosci. **3**, 189 (2006).
[24] I.V. Shadrivov, S.K. Morrison, and Y.S. Kivshar, Opt. Express **14**, 9344 (2006).
[25] D.H. Werner, D.-H. Kwon, I.-C. Khoo, A.V. Kildishev, and V.M. Shalaev, Opt. Express **15**, 3342 (2007).
[26] A. Degiron, J.J. Mock, and D.R. Smith, Opt. Express **15**, 1115 (2007).
[27] D.R. Smith, W.J. Padilla, D.C. Vier, S.C. Nemat-Nasser, and S. Schultz, Phys. Rev. Lett. **84**, 4184 (2000).
[28] R.A. Shelby, D.R. Smith, and S. Schultz, Science **292**, 77 (2001).
[29] J.B. Pendry, A.J. Holden, D.J. Robbins, and W.J. Stewart, IEEE Trans. Microwave Theory Tech. **47**, 2075 (1999).
[30] S. Linden, C. Enkrich, M. Wegener, J. Zhou, T. Koschny, and C.M. Soukoulis, Science **306**, 1351 (2004).
[31] J. Zhou, Th. Koschny, M. Kafesaki, E.N. Economou, J.B. Pendry, and C.M. Soukoulis, Phys. Rev. Lett. **95**, 223902 (2005).
[32] M.W. Klein, C. Enkrich, M. Wegener, C.M. Soukoulis, and S. Linden, Opt. Lett. **31**, 1259 (2006).
[33] S. Zhang, W. Fan, N.C. Panoiu, K.J. Malloy, R.M. Osgood, and S.R.J. Brueck, Phys. Rev. Lett. **95**, 137404 (2005).
[34] U.K. Chettiar, A.V. Kildishev, T.A. Klar, and V.M. Shalaev, Opt. Express **14**, 7872 (2006).
[35] G. Dolling, C. Enkrich, M. Wegener, C.M. Soukoulis, and S. Linden, Opt. Lett. **31**, 1800 (2006).
[36] V.P. Drachev, W. Cai, U. Chettiar, H.-K. Yuan, A.K. Sarychev, A.V. Kildishev, and V.M. Shalaev, Laser Phys. Lett. **3**, 49 (2006).
[37] A.V. Kildishev, W. Cai, U.K. Chettiar, H.-K. Yuan, A.K. Sarychev, V.P. Drachev, and V.M. Shalaev, J. Opt. Soc. Am. B **23**, 423 (2006).

[38] A.K. Sarychev, G. Shvets, and V.M. Shalaev, Phys. Rev. E **73**, 036609 (2006).
[39] S. Zhang, W. Fan, N.C. Panoiu, K.J. Malloy, R.M. Osgood, and S.R. Brueck, Opt. Express **14**, 6778 (2006).
[40] G. Dolling, M. Wegener, C.M. Soukoulis, and S. Linden, Opt. Lett. **32**, 53 (2007).
[41] G. Dolling, M. Wegener, and S. Linden, Opt. Lett. **32**, 551 (2007).
[42] U.K. Chettiar, A.V. Kildishev, H.-K. Yuan, W. Cai, S. Xiao, V.P. Drachev, and V.M. Shalaev, Opt. Lett. **32**, 1671 (2007).
[43] V.A. Podolskiy, A.K. Sarychev, and V.M. Shalaev, J. Nonlinear Opt. Phys. Mater. **11**, 65 (2002).
[44] V. Podolskiy, A. Sarychev, and V. Shalaev, Opt. Express **11**, 735 (2003).
[45] T.A. Klar, A.V. Kildishev, V.P. Drachev, and V.M. Shalaev, IEEE J. Sel. Top. Quantum Electron. **12**, 1106 (2006).
[46] R.A. Depine and A. Lakhtakia, Microwave Opt. Technol. Lett. **41**, 315 (2004).
[47] M. Peccianti and G. Assanto, Opt. Express **15**, 8021 (2007).
[48] E. Schonbrun, M. Tinker, W. Park, and J.-B. Lee, IEEE Photon. Technol. Lett. **17**, 1196 (2005).
[49] N. Fang, H. Lee, C. Sun, and X. Zhang, Science **308**, 534 (2005).
[50] R.J. Blaikie and D.O.S. Melville, J. Opt. A **7**, S176 (2005).
[51] D. Melville and R. Blaikie, Opt. Express **13**, 2127 (2005).
[52] T. Taubner, D. Korobkin, Y. Urzhumov, G. Shvets, and R. Hillenbrand, Science **313**,1595 (2006).
[53] Z. Jacob, L.V. Alekseyev, and E. Narimanov, Opt. Express **14**, 8247 (2006).
[54] A. Salandrino and N. Engheta, Phys. Rev. B **74**, 075103 (2006).
[55] V.A. Podolskiy and E.E. Narimanov, Phys. Rev. B **71**, 201101 (2005).
[56] V.A. Podolskiy, L.V. Alekseyev, and E.E. Narimanov, J. Modern Opt. **52**, 2343, 2005.
[57] R. Wangberg, J. Elser, E.E. Narimanov, and V.A. Podolskiy, J. Opt. Soc. Am. B. **23**, 498 (2006).
[58] A.A. Govyadinov and V.A. Podolskiy, Phys. Rev. B **73**, 155108 (2006).
[59] Z. Liu, S. Durant, H. Lee, Y. Pikus, N. Fang, Y. Xiong, C. Sun, and X. Zhang, Nano Lett. **7**, 403 (2007).
[60] A.A. Zharov, I.V. Shadrivov, and Yu.S. Kivshar, Phys. Rev. Lett. **91**, 037401 (2003).
[61] M. Lapine, M. Gorkunov, and K.H. Ringhofer, Phys. Rev. E **67**, 065601 (2003).
[62] V.M. Agranovich, Y.R. Shen, R.H. Baughman, and A.A. Zakhidov, Phys. Rev. B **69**, 165112 (2004).
[63] N. Mattiucci, G. D'Aguanno, M.J. Bloemer, and M. Scalora, Phys. Rev E **72**, 066612 (2005).
[64] G. D'Aguanno, N. Mattiucci, M.J. Bloemer, and M. Scalora, Phys. Rev. E **73**, 036603 (2006).
[65] I.V. Shadrivov, A.A. Zharov, and Y.S. Kivshar, J. Opt. Soc. Am. B **23**, 529 (2006).
[66] A.K. Popov, V.V. Slabko, and V.M. Shalaev, Laser Phys. Lett. **3**, 293 (2006).
[67] A.K. Popov and V.M. Shalaev, Appl. Phys. B **84**, 131 (2006).
[68] A.K. Popov and V.M. Shalaev, Opt. Lett. **31**, 2169 (2006).
[69] M.V. Gorkunov, I.V. Shadrivov, and Y.S. Kivshar, Appl. Phys. Lett. **88**, 071912 (2006).
[70] A.B. Kozyrev, H. Kim, and D.W. van der Weide, Appl. Phys. Lett. **88**, 264101 (2006).
[71] A.K. Popov, S.A. Myslivets, T.F. George, and V.M. Shalaev, Opt. Lett. **32**, 3044 (2007).
[72] I.V. Shadrivov, A.A. Sukhorukov, Yu.S. Kivshar, A.A. Zharov, A.D. Boardman, and P. Egan, Phys. Rev. E **69**, 016617 (2004).
[73] I.V. Shadrivov, A.A. Sukhorukov, and Yu.S. Kivshar Phys. Rev. E **67**, 057602 (2003).
[74] N. Lazarides and G.P. Tsironis, Phys. Rev. E **71**, 036614 (2005).
[75] I. Kourakis and P.K. Shukla, Phys. Rev. E **72**, 016626 (2005).
[76] I. Shadrivov, N. Zharova, A. Zharov, and Yu. Kivshar, Opt. Express **13**, 1291 (2005).
[77] I.V. Shadrivov and Yu.S. Kivshar, J. Opt. A **7**, S68 (2005).
[78] I.R. Gabitov, R.A. Indik, N.M. Litchinitser, A.I. Maimistov, V.M. Shalaev, and J.E. Soneson, J. Opt. Soc. Am. B **23**, 535 (2006).
[79] A. Alu and N. Engheta, in: G.V. Eleftheriades and K.G. Balmain (eds.), Negative-Refraction Metamaterials; Fundamental Principles and Applications (Wiley, New York, 2005).
[80] N.M. Litchinitser, I.R. Gabitov, and A.I. Maimistov, Phys. Rev. Lett. **99**, 113902 (2007).
[81] A.I. Maĭmistov, I.R. Gabitov, and N.M. Litchinitser, Opt. Spectrosc. **104**, 253 (2008).
[82] A. Alu and N. Engheta, IEEE Trans. Anten. Propag. **51**, 2558 (2003).
[83] A. Alu and N. Engheta, IEEE Trans. Microwave Theor. Tech. **52**, 199 (2004).
[84] N. Engheta and R.W. Ziolkowski, IEEE Trans. Microwave Theor. Tech. **53**, 1535 (2005).
[85] R.W. Ziolkowski, J. Opt. Soc. Am. B **23**, 451 (2006).
[86] N.M. Litchinitser, I.R. Gabitov, A.I. Maimistov, and V.M. Shalaev, Opt. Lett. **32**, 151 (2007).
[87] X. Wang, D.-H. Kwon, D.H. Werner, I.-C. Khoo, A.V. Kildishev, and V.M. Shalaev, Appl. Phys. Lett. **91**, 143122 (2007).
[88] M. Rahm, D. Schurig, D.A. Roberts, S.A. Cummer, D.R. Smith, and J.B. Pendry, aps.arxiv.org/abs/0706.2452.
[89] A.V. Kildishev and V.M. Shalaev, Opt. Lett. **33**, 43 (2008).
[90] H. Chen and C.T. Chan, Appl. Phys. Lett. **90**, 241105 (2007).
[91] A.V. Kildishev and E.E. Narimanov, Opt. Lett. **32**, 3432 (2007).
[92] N.A. Nicorovici, R.C. McPhedran, and G.W. Milton, Phys. Rev. B **49**, 8479 (1994).
[93] A. Alù and N. Engheta, Phys. Rev. E **72**, 016623 (2005).
[94] A. Alù and N. Engheta, Opt. Express **15**, 3318 (2007).
[95] A. Alu and N. Engheta, Opt. Express **15**, 7578 (2007).
[96] G.W. Milton and N.-A.P. Nicorovici, Proc. Roy. Soc. A **462**, 3027 (2006).
[97] N.A. Nicorovici, G.W. Milton, R.C. McPhedran, and L.C. Botten, Opt. Express **15**, 6314 (2007).